and human ESCs [39–41]. Thus, these reports suggest that rat ESCs are readily amenable to gene targeting by homologous recombination using the basic methodology that has proved so effective in mouse ESCs.

Discussion

Rat transgenesis via gene manipulation in ESCs was demonstrated in 2010, marking the beginning of a new era in rat genetics. Although some problems remain in the rat ESC handling, a combination of the methods described in this manuscript as well as newly devised techniques will lead to the discovery of a gold standard method to routinely generate genetically modified rats from ESCs. Recently, not only knockout but also knockin rats have been generated using ZFN-mediated homologous recombination [42]. This knockin strategy will make it possible to introduce temporal control and tissue-specific changes in genes in rat models by combining *Cre/loxP* and an inducible gene expression system. ZFN technology also possesses several advantages, such that the time frame to obtain mutant animals is short, ZFN-mediated homologous recombination in embryos does not require a selection marker, and time-consuming backcrossing is avoided [42]. However, this technology remains expensive to purchase, which is an obstacle for most researchers. In contrast, researchers can apply gene targeting by using ESCs, as is routinely done in mouse research. Therefore, ESC is also required to expand knockout rat lines. There is another advantage of using ESCs when generating transgenic rats. Useless transgenic animals are frequently generated with the conventional method. However, as described in this manuscript, we can choose ESC clones in which a transgene is correctly expressed, leading to the generation of high-quality transgenic rats [36]. Moreover, we can analyze gene function in chimeric animals by using ESCs. Recent reports have shown that this chimeric strategy is effective in identifying gene functions in vivo in terms of developing a more clinically relevant stochastic model [43]. Thus, we speculate that using both the ESC and ZFN strategies will be necessary for routine rat transgenesis.

We now have an opportunity to find new gene functions that have been concealed or questioned in mutant mice. We have accumulated genetic information and a vast amount of research data on physiology and pharmacology in rats. Thus, a combination of these studies will lead to the discovery of new and profound mechanisms of human diseases and the manufacture of medicines to cure patients. Furthermore, rats with their larger sizes make it possible to extract sufficient quantities of samples, such as blood, without killing the animals and to perform difficult surgeries, such as those in brain tissue; all of this emphasizes the advantages of gene-modified rats. We hope that researchers will create many genetically modified rats and open up a powerful new platform for the study of human diseases.

Acknowledgments This work is supported by a Grant-in-Aid from the Third-Term Comprehensive 10-Year Strategy for Cancer Control.

References

1. Brook FA, Gardner RL (1997) The origin and efficient derivation of embryonic stem cells in the mouse. Proc Natl Acad Sci USA 94:5709–5712
2. Evans MJ, Kaufman MH (1981) Establishment in culture of pluripotential cells from mouse embryos. Nature 292:154–156
3. Martin GR (1981) Isolation of a pluripotent cell line from early mouse embryos cultured in medium conditioned by teratocarcinoma stem cells. Proc Natl Acad Sci USA 78:7634–7638
4. Thomson JA, Marshall VS (1998) Primate embryonic stem cells. Curr Top Dev Biol 38:133–165
5. Bradley A, Evans M, Kaufman MH, Robertson E (1984) Formation of germ-line chimaeras from embryo-derived teratocarcinoma cell lines. Nature 309:255–256
6. Robertson E, Bradley A, Kuehn M, Evans M (1986) Germ-line transmission of genes introduced into cultured pluripotential cells by retroviral vector. Nature 323:445–448
7. Koller BH, Hagemann LJ, Doetschman T, Hagaman JR, Huang S, Williams PJ, First NL, Maeda N, Smithies O (1989) Germ-line transmission of a planned alteration made in a hypoxanthine phosphoribosyltransferase gene by homologous recombination in embryonic stem cells. Proc Natl Acad Sci USA 86:8927–8931
8. Gill TJ 3rd, Smith GJ, Wissler RW, Kunz HW (1989) The rat as an experimental animal. Science 245:269–276
9. Jacob HJ (1999) Functional genomics and rat models. Genome Res 9:1013–1016
10. Jacob HJ, Kwitek AE (2002) Rat genetics: attaching physiology and pharmacology to the genome. Nat Rev Genet 3:33–42
11. Aitman TJ, Critser JK, Cuppen E, Dominiczak A, Fernandez-Suarez XM, Flint J, Gauguier D, Geurts AM, Gould M, Harris PC, Holmdahl R, Hubner N, Izsvák Z, Jacob HJ, Kuramoto T, Kwitek AE, Marrone A, Mashimo T, Moreno C, Mullins J, Mullins L, Olsson T, Pravenec M, Riley L, Saar K, Serikawa T, Shull JD, Szpirer C, Twigger SN, Voigt B, Worley K (2008) Progress and prospects in rat genetics: a community view. Nat Genet 40:516–522
12. Jacob HJ, Lazar J, Dwinell MR, Moreno C, Geurts AM (2010) Gene targeting in the rat: advances and opportunities. Trends Genet 26:510–518
13. Brenin D, Look J, Bader M, Hübner N, Levan G, Iannaccone P (1997) Rat embryonic stem cells: a progress report. Transplant Proc 29:1761–1765
14. Buehr M, Nichols J, Stenhouse F, Mountford P, Greenhalgh CJ, Kantachuvesiri S, Brooker G, Mullins J, Smith AG (2003) Rapid loss of Oct-4 and pluripotency in cultured rodent blastocysts and derivative cell lines. Biol Reprod 68:222–229
15. Demers SP, Yoo JG, Lian L, Therrien J, Smith LC (2007) Rat embryonic stem-like (ES-like) cells can contribute to extraembryonic tissues in vivo. Cloning Stem Cells 9:512–522
16. Fändrich F, Dresske B, Bader M, Schulze M (2002) Embryonic stem cells share immune-privileged features relevant for tolerance induction. J Mol Med 80:343–530
17. Vassilieva S, Guan K, Pich U, Wobus AM (2000) Establishment of SSEA-1- and Oct-4-expressing rat embryonic stem-like cell

lines and effects of cytokines of the IL-6 family on clonal growth. Exp Cell Res 258:361–373
18. Ueda S, Kawamata M, Teratani T, Shimizu T, Tamai Y, Ogawa H, Hayashi K, Tsuda H, Ochiya T (2008) Establishment of rat embryonic stem cells and making of chimera rats. PLoS One 3:e2800
19. Zan Y, Haag JD, Chen KS, Shepel LA, Wigington D, Wang YR, Hu R, Lopez-Guajardo CC, Brose HL, Porter KI, Leonard RA, Hitt AA, Schommer SL, Elegbede AF, Gould MN (2003) Production of knockout rats using ENU mutagenesis and a yeast-based screening assay. Nat Biotechnol 21:645–651
20. Kitada K, Ishishita S, Tosaka K, Takahashi R, Ueda M, Keng VW, Horie K, Takeda J (2007) Transposon-tagged mutagenesis in the rat. Nat Methods 4:131–133
21. Lu B, Geurts AM, Poirier C, Petit DC, Harrison W, Overbeek PA, Bishop CE (2007) Generation of rat mutants using a coat color-tagged Sleeping Beauty transposon system. Mamm Genome 18:338–346
22. Cozzi J, Anegon I, Braun V, Gross AC, Merrouche C, Cherifi Y (2009) Pronuclear DNA injection for the production of transgenic rats. Methods Mol Biol 561:73–88
23. Geurts AM, Cost GJ, Freyvert Y, Zeitler B, Miller JC, Choi VM, Jenkins SS, Wood A, Cui X, Meng X, Vincent A, Lam S, Michalkiewicz M, Schilling R, Foeckler J, Kalloway S, Weiler H, Ménoret S, Anegon I, Davis GD, Zhang L, Rebar EJ, Gregory PD, Urnov FD, Jacob HJ, Buelow R (2009) Knockout rats via embryo microinjection of zinc-finger nucleases. Science 325:433
24. Izsvák Z, Fröhlich J, Grabundzija I, Shirley JR, Powell HM, Chapman KM, Ivics Z, Hamra FK (2010) Generating knockout rats by transposon mutagenesis in spermatogonial stem cells. Nat Methods 7:443–445
25. Mashimo T, Takizawa A, Voigt B, Yoshimi K, Hiai H, Kuramoto T, Serikawa T (2010) Generation of knockout rats with X-linked severe combined immunodeficiency (X-SCID) using zinc-finger nucleases. PLoS One 5:e8870
26. Ménoret S, Iscache AL, Tesson L, Rémy S, Usal C, Osborn MJ, Cost GJ, Brüggemann M, Buelow R, Anegon I (2010) Characterization of immunoglobulin heavy chain knockout rats. Eur J Immunol 40:2932–2941
27. Buehr M, Meek S, Blair K, Yang J, Ure J, Silva J, McLay R, Hall J, Ying QL, Smith A (2008) Capture of authentic embryonic stem cells from rat blastocysts. Cell 135:1287–1298
28. Li P, Tong C, Mehrian-Shai R, Jia L, Wu N, Yan Y, Maxson RE, Schulze EN, Song H, Hsieh CL, Pera MF, Ying QL (2008) Germline competent embryonic stem cells derived from rat blastocysts. Cell 135:1299–1310
29. Kawamata M, Ochiya T (2010) Establishment of embryonic stem cells from rat blastocysts. Methods Mol Biol 597:169–177
30. Ying QL, Wray J, Nichols J, Batlle-Morera L, Doble B, Woodgett J, Cohen P, Smith A (2008) The ground state of embryonic stem cell self-renewal. Nature 453:519–523
31. Li W, Wei W, Zhu S, Zhu J, Shi Y, Lin T, Hao E, Hayek A, Deng H, Ding S (2009) Generation of rat and human induced pluripotent stem cells by combining genetic reprogramming and chemical inhibitors. Cell Stem Cell 4:16–19
32. Hirabayashi M, Kato M, Sanbo M, Kobayashi T, Hochi S, Nakauchi H (2010) Rat transgenesis via embryonic stem cells electroporated with the Kusabira-orange gene. Mol Reprod Dev 77:474
33. Takahama Y, Ochiya T, Sasaki H, Baba-Toriyama H, Konishi H, Nakano H, Terada M (1998) Molecular cloning and functional analysis of cDNA encoding a rat leukemia inhibitory factor: towards generation of pluripotent rat embryonic stem cells. Oncogene 16:3189–3196
34. Hirabayashi M, Kato M, Kobayashi T, Sanbo M, Yagi T, Hochi S, Nakauchi H (2010) Establishment of rat embryonic stem cell lines that can participate in germline chimerae at high efficiency. Mol Reprod Dev 77:94
35. Kobayashi T, Yamaguchi T, Hamanaka S, Kato-Itoh M, Yamazaki Y, Ibata M, Sato H, Lee YS, Usui J, Knisely AS, Hirabayashi M, Nakauchi H (2010) Generation of rat pancreas in mouse by interspecific blastocyst injection of pluripotent stem cells. Cell 142:787–799
36. Kawamata M, Ochiya T (2010) Generation of genetically modified rats from embryonic stem cells. Proc Natl Acad Sci USA 107:14223–14228
37. Tong C, Li P, Wu NL, Yan Y, Ying QL (2010) Production of p53 gene knockout rats by homologous recombination in embryonic stem cells. Nature 467:211–213
38. Meek S, Buehr M, Sutherland L, Thomson A, Mullins JJ, Smith AJ, Burdon T (2010) Efficient gene targeting by homologous recombination in rat embryonic stem cells. PLoS One 5:e14225
39. Thomas KR, Capecchi MR (1987) Site-directed mutagenesis by gene targeting in mouse embryo-derived stem cells. Cell 51:503–512
40. Doetschman T, Maeda N, Smithies O (1988) Targeted mutation of the Hprt gene in mouse embryonic stem cells. Proc Natl Acad Sci USA 85:8583–8587
41. Zwaka TP, Thomson JA (2003) Homologous recombination in human embryonic stem cells. Nat Biotechnol 21:319–321
42. Cui X, Ji D, Fisher DA, Wu Y, Briner DM, Weinstein EJ (2011) Targeted integration in rat and mouse embryos with zinc-finger nucleases. Nat Biotechnol 29:64–67
43. Zhou Y, Rideout WM 3rd, Zi T, Bressel A, Reddypalli S, Rancourt R, Woo JK, Horner JW, Chin L, Chiu MI, Bosenberg M, Jacks T, Clark SC, Depinho RA, Robinson MO, Heyer J (2010) Chimeric mouse tumor models reveal differences in pathway activation between ERBB family- and KRAS-dependent lung adenocarcinomas. Nat Biotechnol 28:71–78

Inhibition of Stabilin-2 elevates circulating hyaluronic acid levels and prevents tumor metastasis

Yoshikazu Hirose[a,1], Eiko Saijou[a,1], Yasuyoshi Sugano[a,1], Fumitaka Takeshita[b], Satoshi Nishimura[c,d], Hidenori Nonaka[a], Yen-Rong Chen[a], Keisuke Sekine[a], Taketomo Kido[a], Takashi Nakamura[e], Shigeaki Kato[e], Toru Kanke[f], Koji Nakamura[f], Ryozo Nagai[c,d,g], Takahiro Ochiya[b], and Atsushi Miyajima[a,2]

[a]Laboratory of Cell Growth and Differentiation and [e]Laboratory of Nuclear Signaling, Institute of Molecular and Cellular Biosciences, University of Tokyo, Tokyo 113-0032, Japan; [b]Division of Molecular and Cellular Medicine, National Cancer Center Research Institute, Tokyo 104-0045, Japan; [c]Department of Cardiovascular Medicine, [d]Translational Systems Biology and Medicine Initiative, and [g]Global Center of Excellence Program, Comprehensive Center of Education and Research for Chemical Biology of the Diseases, University of Tokyo, Tokyo 113-8655, Japan; and [f]LivTech Inc., Kanagawa 216-0001, Japan

Edited by Joan Massagué, Memorial Sloan-Kettering Cancer Center, New York, NY, and approved February 3, 2012 (received for review October 31, 2011)

Hyaluronic acid (HA) has been implicated in the proliferation and metastasis of tumor cells. However, most previous studies were conducted on extracellular matrix or pericellular HA, and the role of circulating HA in vivo has not been studied. HA is rapidly cleared from the bloodstream. The scavenger receptor Stabilin-2 (Stab2) is considered a major clearance receptor for HA. Here we report a dramatic elevation in circulating HA levels in Stab2-deficient mice without any overt phenotype. Surprisingly, the metastasis of B16F10 melanoma cells to the lungs was markedly suppressed in the Stab2-deficient mice, whereas cell proliferation was not affected. Furthermore, administration of an anti-Stab2 antibody in Stab2$^+$ mice elevated serum HA levels and prevented the metastasis of melanoma to the lung, and also suppressed spontaneous metastasis of mammary tumor and human breast tumor cells inoculated in the mammary gland. Administration of the antibody or high-dose HA in mice blocked the lodging of melanoma cells to the lungs. Furthermore, HA at high concentrations inhibited the rolling/tethering of B16 cells to lung endothelial cells. These results suggest that blocking Stab2 function prevents tumor metastasis by elevating circulating HA levels. Stab2 may be a potential target in antitumor therapy.

cancer | hyaluronan | imaging | antibody therapy | sinusoid

Scavenger receptors mediate the endocytosis of metabolic waste products produced under normal and pathological conditions, as well as harmful foreign substances, such as bacterial debris absorbed in the gut. The liver functions as a major filter to eliminate such molecules from the circulation. Liver-specific capillaries known as sinusoids are vital to this function; for example, more than 90% of circulating hyaluronic acid (HA) is cleared by liver sinusoids (1). Sinusoidal walls consist of hepatic sinusoid endothelial cells (HSECs), stellate cells, and liver resident macrophages known as Kupffer cells. HSECs and Kupffer cells express various types of scavenger receptors to fulfill the filter functions. Among those scavenger receptors, Stabilin-1 (Stab1, also known as FEEL-1 and CLEVER-1) and Stabilin-2 (Stab2, also known as FEEL-2 and HARE) are structurally related, exhibiting 55% homology at the protein level, and expressed on HSECs (2).

Stab1 and Stab2 are large type I transmembrane glycoproteins containing four domains with EGF-like repeats, seven fasciclin-1 domains, and an X-link domain (3). Despite these two glycoproteins' structural similarity, the spectrum of their ligands differs significantly. Stab1 is expressed on lymphatic vessels and macrophages as well as HSEC and binds to acetylated low-density lipoprotein (ac-LDL), secreted protein acidic and rich in cysteine, placental lactogen, growth differentiation factor 15, and Gram-positive and Gram-negative bacteria, but not to HA (2, 4–8). It also mediates leukocyte trafficking (9). Stab2 is expressed on the sinusoid endothelium in the liver, spleen, and lymph nodes and has been used as a specific marker for HSECs (10). It binds to and mediates the endocytosis of HA, advanced glycation end products-modified protein, and heparin in addition to ac-LDL, growth differentiation factor 15, and bacteria (2, 4). Stab2 also recognizes membrane phosphatidylserine of apoptotic cells (11). Previous studies found that unlabeled chondroitin sulfate inhibited the uptake of ^{125}-I-HA (12), and that ac-LDL binding to Stab2 was partially competed by heparin and dextran sulfate, but not competed by HA (13). These findings suggest that the HA binding site overlaps with the binding site of chondroitin sulfate but differs from the binding sites of ac-LDL, heparin, and dextran sulfate.

HA is a glycosaminoglycan of the extracellular matrix consisting of tandem repeats of D-glucuronic acid and *N*-acety-D-glucosamine. HA is abundant in the umbilical cord, articular joints, cartilage, and vitreous humor (14). It has been implicated in various physiological functions, including lubrication, water homeostasis, filtering effects, regulation of plasma protein distribution, angiogenesis, wound healing, and chondrogenesis (15). Signal transduction and functions of HA differ depending on molecular size; for example, high molecular weight HA suppresses angiogenesis, whereas HA fragments stimulate angiogenesis (16).

HA interacts with various cell surface receptors, including CD44, Lyve-1, TLRs, RHAMM, and Stab2 (17, 18). CD44, the most extensively characterized of these receptors, is expressed at varying levels in most immune cells and is involved in their rolling and extravasation via HA displayed on endothelial cells (ECs) (19). CD44 is also implicated in tumorigenesis and a marker for cancer stem cells (reviewed in ref. 20). Lyve-1 is structurally related to CD44 and is expressed in lymphatic vessels as well as in HSECs (21). TLR2 and TLR4 bind to HA or a complex of HA and HA-binding protein (18, 22); however, none of the mice deficient for CD44, Lyve-1, or TLRs have been shown to affect circulating HA levels in vivo. Although Stab1 and Stab2 are structurally related scavenger receptors with the HA-binding link domain, only Stab2 binds HA, and thus it has been considered the primary scanvenger receptor for HA (2, 3, 5).

HA, HA synthases (HAS), hyaluronidases, and HA receptors have been implicated in various tumors, including carcinomas, lymphomas, and melanocytic and neuronal tumors (23, 24). Overexpression and knockdown of HAS and hyaluronidases

Author contributions: Y.H., E.S., Y.S., H.N., and A.M. designed research; Y.H., E.S., Y.S., F.T., S.N., Y.-R.C., K.S., T. Kido, T.N., S.K., T. Kanke, K.N., R.N., and T.O. performed research; Y.H., E.S., Y.S., F.T., S.N., and A.M. analyzed data; and Y.H., E.S., and A.M. wrote the paper.

The authors declare no conflict of interest.

This article is a PNAS Direct Submission.

[1]Y.H., E.S., and Y.S. contributed equally to this work.

[2]To whom correspondence should be addressed. E-mail: miyajima@iam.u-tokyo.ac.jp.

This article contains supporting information online at www.pnas.org/lookup/suppl/doi:10.1073/pnas.1117560109/-/DCSupplemental.

have revealed that HA positively regulates proliferation, invasion, cell motility, multidrug resistance, and epithelial–mesenchymal transition in many tumor cell lines in vitro and in vivo (reviewed in ref. 23). Furthermore, an HAS inhibitor, 4-methylubelliferon, has been shown to decrease tumor proliferation and metastasis (25, 26).

Despite the importance of HA in tumorigenesis, assessing the role of circulating HA in tumor progression is difficult, because HA administered in the body is rapidly eliminated from the bloodstream (1). In this study, we generated Stab2 KO mice in which plasma HA levels were significantly elevated without any overt phenotype. Unexpectedly, tumor metastasis was markedly suppressed in these mice. We also found that administration of an anti-Stab2 antibody in WT mice elevated circulating HA levels and prevented tumor metastasis. Finally, we found that administration of a high dose of HA prevented the attachment of melanoma cells to the lungs in vivo and in vitro, and examined a possible link between circulating HA levels and tumor metastasis.

Results

Elevation of Circulating HA Levels in Stab2 KO Mice. To address the physiological roles of Stab2 in vivo, we generated a Stab2 KO mouse line by replacing most of the first exon, including the ATG initiation codon and the first intron, with the LacZ and neomycin resistance genes (Figs. S1 *A–C*). The lack of Stab2 expression in KO mice was confirmed by RT-PCR and immunostaining (Figs. S1 *D* and *H* and S2*D*), Stab2-deficient mice were born according to the Mendelian ratio, grew normally, and showed no apparent abnormalities (Fig. S1 *E* and *F*). Histological analyses revealed no significant changes (Fig. S1*G*). Staining of liver sections with the anti-CD31 antibody, which binds HSECs as well as other types of ECs in the liver, demonstrated normal development of HSECs (Fig. S1*H*). Furthermore, we found no significant differences in conventional diagnostic markers for functions of the pancreas, liver, and kidney (Table S1). These results indicate that Stab2 is dispensable for normal development and viability in mice.

Given that Stab2 is a known scavenger receptor that binds and eliminates from the circulation various substances, including HA, ac-LDL, and heparin (4, 27, 28), we assessed the circulating levels of these substances in Stab2 KO mice. Although serum levels of ac-LDL and heparin were unchanged in the Stab2 KO mice (Table S1), serum HA levels were dramatically increased, by as much as 59-fold over control values (Fig. 1*A*). Because HA's molecular size affects its function (16), we next analyzed the molecular size of serum HA by electrophoresis using Stains-All (which stains negatively charged molecules), and estimated it as ~40 kDa (Fig. S1*J*). Given that >90% of the circulating HA is cleared by HSECs (1), and that Stab2 is specifically expressed in HSECs, we examined whether the high serum HA levels in Stab2 KO mice were due to impaired endocytosis. We prepared HSECs from WT and Stab2 KO mice and quantitatively evaluated their endocytotic activity based on the internalization of FITC-labeled HA and DiI-labeled ac-LDL (DiI-Ac-LDL) (Fig. 1*B* and *C* and Fig. S1 *K* and *L*). Although there was no significant difference in the internalization of DiI-Ac-LDL between WT and Stab2 KO mice, the internalization of HA into Stab2-deficient HSECs was markedly decreased, to only ~8% of the WT level. We also examined the expression of other HA receptors (CD44 and Lyve-1) and HA synthases (HAS1, HAS2, and HAS3) that can potentially affect HA levels, but found no significant changes in the Stab2 KO mice (Fig. S2 *A* and *B*). These results provide clear evidence that Stab2 is the major clearance receptor for HA in the body.

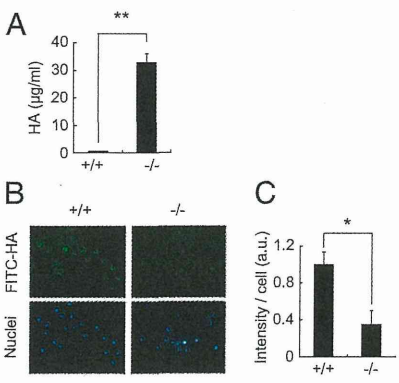

Fig. 1. Serum HA levels and internalization of HA in Stab2-deficient cells. (*A*) Serum HA levels in WT ($^{+/+}$) and homozygous ($^{-/-}$) littermates ($n = 3$; $^{**}P < 0.01$). (*B*) Internalization of FITC-HA in Percoll-purified HSECs from Stab2$^{+/+}$ and Stab2$^{-/-}$ littermates. (*Upper*) Fluorescence of FITC-HA incorporated into cells. (*Lower*) Hoechst 33342 staining. (*C*) Quantification of FITC fluorescence intensity ($n = 4$; $^{*}P < 0.05$).

Metastasis of Melanoma Cells Is Suppressed in Stab2 KO Mice. The elevation in serum HA levels in Stab2 KO mice prompted us to examine whether the lack of Stab2 has any effects on tumorigenesis. B16 melanoma cells are known to form tumor nodules in the lung when injected i.v. We administered B16F10 cells i.v. in littermates of Stab2$^{+/+}$ and Stab2$^{-/-}$ mice. After 14 d, numerous black nodules had formed on the lung surfaces of the Stab2$^{+/+}$ mice, but surprisingly, nodular formation was markedly reduced in Stab2$^{-/-}$ mice (Fig. 2 *A* and *B*). In contrast, tumor formation resulting from the s.c. inoculation of melanoma cells did not differ significantly between the Stab2$^{+/+}$ and Stab2$^{-/-}$ mice (Fig. 2*C*). Moreover, our in vitro experiments showed that the proliferation of B16F10 cells was not affected by HA, and a cell cycle analysis of B16F10 cells recovered from lung tumors revealed no difference between the Stab2 KO and WT mice (Fig. S3*A*). These results indicate that the metastasis, but not the proliferation, of melanoma cells was affected by the lack of Stab2.

To analyze the early stages of metastasis, we also conducted imaging in vivo, because the nodules of B16F10 cells at day 7 were too small to count. B16F10 cells were stably transfected with the firefly luciferase gene to generate B16F10-luc-G5 cells,

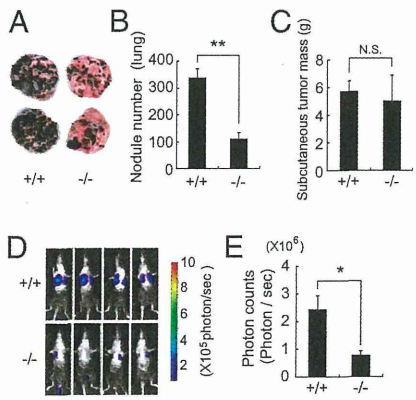

Fig. 2. Homing of B16F10 melanoma to the lungs in Stab2 KO mice. B16F10 cells (5×10^5) were injected via the tail vein in Stab2$^{+/+}$ and Stab2$^{-/-}$ littermates. (*A*) Metastatic nodules formed on the lungs at day 14 after the injection. (*B*) Numbers of nodules formed on the lungs were counted manually ($^{+/+}$, $n = 9$; $^{-/-}$, $n = 6$; $^{**}P < 0.01$). (*C*) Size of tumors formed by s.c. inoculated melanoma cells at day 21 [$^{+/+}$, $n = 8$; $^{-/-}$, $n = 6$; $^{*}P > 0.05$ (not significant)]. (*D*) Metastasis of i.v. injected B16F10-luc-G5 cells measured by luminescence using IVIS in vivo imaging at day 7. (*E*) Quantification of photon counts in *C* ($^{+/+}$, $n = 6$; $^{-/-}$, $n = 5$; $^{*}P < 0.05$).

which were then injected i.v. into littermates of Stab2$^{+/+}$ and Stab2$^{-/-}$ mice. After 7 d, tumor metastasis was measured based on the luminescence of luciferase. Photon counts were significantly decreased in the Stab2$^{-/-}$ mice, indicating inhibition of metastasis at an early stage (Fig. 2 *D* and *E*).

Administration of Anti-Stab2 Antibody Increases Serum HA Levels and Prevents Tumor Metastasis. We next investigated whether Stab2 functions could be blocked by an anti-Stab2 antibody in vivo. We generated several mAbs against the extracellular domain of Stab2 by immunizing rats with BaF3 cells expressing Stab2 and one of them (#34-2, ref. 10) was found to inhibit HA binding to Stab2 as assessing by internalization of FITC-labeled HSECs in vitro (Fig. 3*A*). To test whether that anti-Stab2 mAb has any effect on the plasma HA level in vivo, we injected it i.p. into C57BL/6 mice every 3 d and monitored serum HA levels. Within 3 d of the first injection, serum HA levels were increased in all of the mice given the anti-Stab2 mAb, but not in the mice treated with rat IgG (Fig. 3*B*). We obtained the same results using SCID mice (Fig. 4 *A* and *J*). These findings clearly indicate that the anti-Stab2 mAb effectively increased plasma HA levels by inhibiting Stab2 function in vivo. To examine whether this mAb prevents tumor metastasis, we injected mice with either anti-Stab2 mAb or control rat IgG, followed 2 d later by i.v. injection of B16F10 cells. The anti-Stab2 mAb significantly suppressed metastasis (Fig. 3 *C* and *D*). Taken together, these results indicate that the anti-Stab2 mAb elevates circulating HA levels by blocking the clearance of HA in HSECs, and that serum HA levels are inversely correlated with tumor metastasis.

Because the anti-Stab2 mAb elevated plasma HA levels in immune deficient mice, we investigated its effect on spontaneous metastasis by multiple cancer cells in SCID mice. To do so, we transplanted MDA-MB-231-luc-D3H2LN cells (human mammary gland adenocarcinoma cells expressing luciferase) into the abdominal mammary glands of SCID mice. After 21 d, tumor metastasis in the upper body, including the brachial lymph nodes, was evaluated by luminescence analysis. The number of photons derived from metastasized cells in the upper body was significantly reduced in the mice treated with the anti-Stab2 mAb (Fig. 4 *A–D*). We also transplanted 4T1-LucNeo-1H mouse mammary tumor cells expressing luciferase into the mammary fad pads of the mice. Starting at 2 d after tumor injection, each animal was given either anti-Stab2 mAb or rat IgG every 3 d. At 3 wk after the start of antibody treatment, metastatic luminescence signals and the numbers of histological lesions in the lung were reduced in the anti-Stab2 mAb-treated mice. Given the lack of significant difference in the size of primary tumors (Fig. 4 *E–L*), anti-Stab2 mAb can be considered to inhibit spontaneous metastasis.

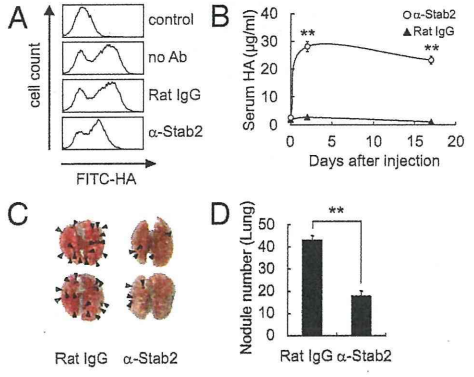

Fig. 3. Inhibition of HA clearance and metastasis by anti-Stab2 mAb. (*A*) HSECs were incubated with anti-Stab2 mAb or rat IgG, and the cell internalization of FITC-HA was analyzed by flow cytometry. (*B*) Anti-Stab2 mAb or rat IgG (3 mg/kg body weight) was administered i.p. to C57BL/6 mice on days 0, 3, and 17, and serum HA levels were measured ($n = 5$; $^{**}P < 0.01$). (*C*) At 2 d after the i.p. administration of anti-Stab2 mAb or control IgG, 5×10^4 B16F10 cells were injected i.v. via the tail vein. Anti-Stab2 mAb or control IgG was administered every 3 d. The lungs at 14 d are shown. Arrowheads indicate nodules of B16F10 cells. (*D*) The number of nodules formed on the lungs were counted manually ($n = 10$; $^{**}P < 0.01$). α-Stab2 denotes anti-Stab2 mAb.

Examination of Possible Mechanisms for Inhibition of Metastasis. To investigate the inhibitory mechanism of metastasis observed in the Stab2 KO and anti-Stab2 mAb-treated mice, we first analyzed whether HA affects tumor cells in vitro. We evaluated the effects of a 31-kDa HA (similar in size to HA in circulation; Fig. S1*J*), on cell proliferation, apoptosis induced by hydrogen peroxide, migration, and invasion into the basal membrane. None of these assays demonstrated any significant effect of HA on tumor cells at various concentrations (Fig. S3 *A–E*).

Because the proliferation as well as metastasis of tumors is under surveillance by the immune system, and HA has been implicated in the immune system, we examined the immune cells of Stab2 KO mice for any changes. We found no significant differences in fractions of regulatory T cells, NK cells, macrophages, and myeloid-derived suppressor cells in bone marrow, peripheral blood, and spleen in Stab2 KO mice compared with WT mice (Fig. S4*A*). In addition, we found no alterations in serum levels of TNF-α, IFN-γ, IL-2, IL-4, IL-6 IL-10, and IL-17A (Fig. S4*B*), or in the activation of macrophages in vivo and sensitivity to i.p. LPS (Figs. S2*E* and S4*C*). These results showing no significant alterations in the immune system in Stab2 KO mice suggest that the immune system may not be directly involved in the inhibition of tumor metastasis.

Attachment of Melanoma Cells to the Lungs Is Prevented by an Increase in Plasma HA. Intravenously injected melanoma cells are thought to roll through the bloodstream and lodge in the lungs, where they proliferate. Our finding that the melanoma cells injected s.c. in Stab2 KO mice formed tumors as large as those seen in their WT littermates (Fig. 2*C*) suggests that the homing of i.v. injected tumor cells to the lungs might be altered in the mutant mice. To analyze the attachment of melanoma cells to the lung in vivo, we inoculated B16F10-luc-G5 cells i.v. After 6 h, mice were perfused with PBS via the portal vein to remove blood cells from the tissues, and luciferase activity in the lungs was evaluated. The luciferase activity in the lungs was significantly decreased in Stab2 KO mice and in mice treated with the anti-Stab2 mAb compared with WT mice and rat IgG-treated mice (Fig. 5 *A* and *B*). These results indicate that tumor metastasis was prevented at an early stage of penetration in the lungs.

Because plasma HA level has been suggested to be involved in the metastasis of melanoma cells, and HA binds to cell surface molecules such as CD44, we investigated whether HA mediates the attachment of tumor cells to tissues. We first tested the binding of melanoma cells to HA by plating B16F10 cells on an HA-coated plate, and found that the cells attached to the plate via HA (Fig. S3*F*). Adding HA at the concentration found in Stab2 KO mouse sera inhibited the binding of B16F10 to the HA-coated plate. This finding suggests that the increased plasma HA in the mutant mice inhibits metastasis by preventing the attachment of melanoma cells to the lung via HA.

We also investigated whether HA prevents the attachment of B16F10 cells to the lung. Although i.v. injected HA is rapidly cleared from the bloodstream (1), we found that a very high dose of HA administered via the tail vain elevated the serum HA level for several hours (Fig. 5*C*). Thus, we injected HA at a dose of 20 mg/kg body weight every 8 h for 24 h to increase the plasma HA level, and then transplanted B16F10-luc-G5 cells. At 6 h after B16F10-luc-G5 cell transplantation, luciferase activity in the lungs was significantly reduced, whereas the serum

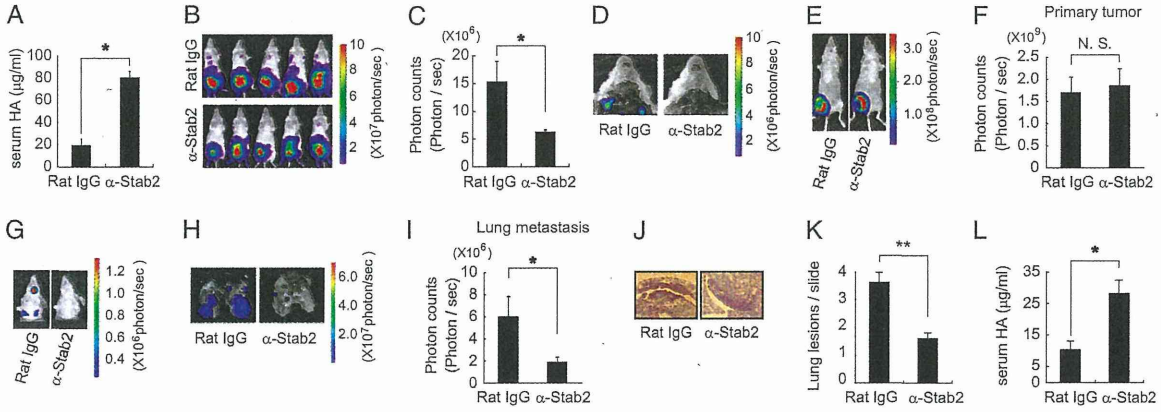

Fig. 4. Anti-Stab2 antibody prevents spontaneous metastasis of human and mouse mammary tumor cells in SCID mice. (*A*) SCID mice were i.p. injected with anti-Stab2 mAb or rat IgG (3 mg/kg), and serum HA levels were measured at 7 d after the injection ($n = 5$; $^*P < 0.05$). (*B*) MDA-MB-231-luc-D3H2LN cells were grafted in the mammary gland of SCID mice injected i.p. with anti-Stab2 mAb or control IgG (3 mg/kg). Luminescence was measured by IVIS at day 21. (*C*) Quantification of photon counts in the upper body at day 21 ($n = 5$; $^*P < 0.05$). (*D*) Luminescence of the opened thorax in *B*. (*E*) Mouse 4T1-LucNeo-1H mammary tumor cells were grafted into a mammary fat pad of the mice. At 2 d after tumor injection, each animal was given anti-Stab2 mAb or Rat IgG i.p. every 3 d, for a total of seven injections. Luminescence of primary tumors was measured by IVIS at day 21. (*G*) For the detection of signals from metastatic regions, the lower part of each animal was shielded with black paper before reimaging, to minimize bioliminescence from primary tumor. At the end of the experiment (day 21), ex vivo imaging was performed on collected lungs. Control group mice exhibited spontaneous lung metastasis. (*F*, *H*, and *I*) Quantification of bioluminescence emitted from primary tumors on mice and lung metastatic regions at the end of the experiment. Data represent mean ± SD ($n = 4$; $^*P < 0.05$ vs. other groups). (*J*) H&E-stained sections of spontaneous lung metastasis lesions at day 21. (*K*) Quantification of lung lesions in *J*. Data represent mean values ($n = 32$; $^{**}P < 0.01$ vs. other groups). (*L*) Serum HA levels measured at the end of the experiment ($n = 4$; $^*P < 0.05$). α-Stab2 denotes anti-Stab2 mAb.

HA level remained elevated in those mice pretreated with HA (Fig. 5 *D* and *E*).

Finally, to prove that increased HA level decreases the arrest of tumor cells in lung capillaries, we performed in vitro rolling/tethering assays using a VenaEC system. Pulmonary ECs from WT mice were cultured on VenaEC substrates and connected to a microfluidic device. Rolling/tethering between pulmonary cells and B16 melanoma cells under share stress was observed (Fig. 5*F*). At a low HA concentration (0.55 μg/mL, similar to Stab2$^{+/+}$ serum levels), B16 melanoma cells were tethered to pulmonary

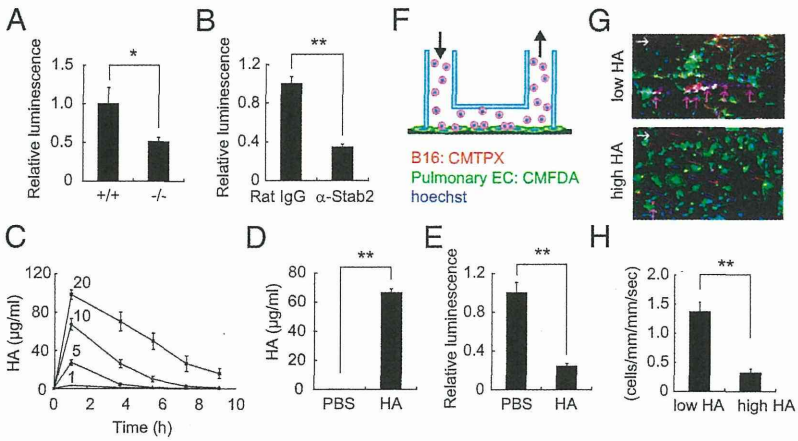

Fig. 5. HA inhibits attachment of B16F10 cells. (*A*) B16F10-luc-G5 cells (1.5×10^6) were injected into the tail vein of Stab2$^{+/+}$ and Stab2$^{-/-}$ mice, and 6 h later, the mice were perfused with PBS via the portal vein to remove blood cells from tissues. The B16F10-luc-G5 cells remaining in the lungs were detected by luciferase analysis ($^{+/+}$, $n = 6$; $^{-/-}$, $n = 7$; $^*P < 0.05$). (*B*) At 2 d after the i.p. administration of anti-Stab2 or rat IgG, B16F10-luc-G5 cells (1.5×10^6) were injected into the tail vein. At 6 h later, the injection cells remaining in the lungs were detected by luciferase analysis as in *A* (rat IgG, $n = 5$; $^{-/-}$, $n = 6$; $^{**}P < 0.01$). (*C*) HA at doses of 1, 5, 10, and 20 mg/kg was injected i.v., and serum HA levels were measured serially ($n = 4$). (*D*) HA at 20 mg/kg or an equal volume of PBS was injected i.v. every 8 h. At 24 h after the first HA injection, B16F10-luc-G5 cells (1.5×10^6) were injected into the tail vein with 20 mg/kg of HA. After 6 h, serum samples were collected, and plasma HA levels were analyzed at the end of experiment ($n = 8$; $^{**}P < 0.01$). (*E*) Cells remaining in the lungs were detected based on luciferase activity at *D* as in *A* ($n = 8$; $^{**}P < 0.01$). (*F*) Schematic diagram of the VenaEC system (Cellix). (*G*) Rolling and/or tethering of B16 melanoma cells onto pulmonary ECs using the VenaEC system. Pulmonary ECs from 6-d-old WT (C57BL/6) mice were isolated, cultured, and stained with 5 μM CMFDA (green) and 10 μM Hoechst 33342 (blue). B16F10 cells were stained with 5 μM CMTPX (red) and 10 μM Hoechst (blue). The pulmonary cell chamber was connected to a microfluidic device, and perfusion for 5 min with VL medium containing stained B16F10 cells at 0.7 dynes/cm^2 was performed during confocal observation of cell kinetics. Representative images of B16 melanoma cells with low (0.55 μg/mL) and high (33 μg/mL) HA concentrations are shown (Movies S1 and S2). White arrows denote flow directions, and red arrows indicate rolling and/or tethering B16F10 cells. (*H*) Quantification of rolling/tethering to the pulmonary ECs. The numbers of rolling/ tethering B16F10 cells were counted. Note that HA at high concentrations inhibited the rolling/tethering of melanoma cells onto pulmonary endothelium ($n = 20$ images from five experiments; $^*P < 0.05$). (Scale bar: 100 μm.) α-Stab2 denotes anti-Stab2 mAb.

cells. In contrast, at a high HA concentration (33 μg/mL, similar to Stab2$^{-/-}$ serum levels), tethering was significantly reduced (Fig. 5 *G* and *H* and Movies S1 and S2). These results indicate that a high level of HA in the circulation prevents the attachment of melanoma cells to the lung.

Discussion

In this study, using Stab2 KO mice and an anti-Stab2 mAb, we provide several lines of evidence indicating that Stab2 is the major clearance receptor for circulating HA. This finding is consistent with the results of a previous in vitro study showing that Stab2, not its homolog Stab1, is the major clearance receptor for HA (5), as well as a recent study using Stab1 and Stab2 KO mice (2). In addition, KO mice deficient in either Lyve1 or Stab1 showed no change in serum HA levels (2, 29), further supporting this idea. Although Stab2 is known to bind other molecules, such as ac-LDL and heparin, serum levels of ac-LDL and heparin were not increased in the Stab2 KO mice, and the internalization of ac-LDL into Stab2-deficient HSECs was normal, indicating that those molecules are cleared by other scavenger receptors, such as Stab1. Therefore, we conclude that Stab2 is the bona fide clearance receptor for circulating HA in vivo.

An unexpected finding—and perhaps the most important result of this study—is the markedly reduced metastasis of melanoma cells in the Stab2 KO mice. Furthermore, i.p. administration of the blocking mAb for Stab2 also increased the serum concentration of HA and inhibited tumor metastasis in the Stab2$^{+/+}$ mice at levels comparable to those in Stab2 KO mice (Fig. 3). The KO mice were fertile, developed normally, and exhibited no hematological or histological changes except for the increased serum HA level (Fig. S1 and Table S1). Although Stab2 has multiple ligands, only HA levels were altered in the Stab2 KO mice, and the anti-Stab2 mAb caused phenotypes similar to those in the Stab2 KO mice. Thus, we focused on HA to investigate the mechanism preventing metastasis, and carried out various experiments in vitro and in vivo. Our in vitro experiments indicated that HA did not affect the proliferation, migration, and invasion of B16F10 cells (Fig. S3 *A*–*E*). Moreover, the weights of tumors formed by s.c. transplanted melanoma cells, as well as the cell cycle status of i.v. injected melanoma cells, were not changed in the Stab2 KO mice, indicating that the lack of Stab2 does not affect tumor proliferation in vivo (Fig. 2*C* and Fig. S3*B*). Likewise, mammary tumor cells formed primary tumors in abdominal fat pads, but tumor formation in the lymph nodes or lung was severely suppressed by anti-Stab2 mAb (Fig. 4). These results strongly suggest that tumor metastasis is prevented by a mechanism other than proliferation.

Tumorigenesis is controlled by the immune system, and the role of HA in the immune system has been studied extensively. Of note, HA binds to TLR2 and TLR4, which play important roles in innate immunity (18). We examined several parameters of the immune system, focusing first on macrophage functions, given that HA has been shown to alter immune responses via TLR4 that binds to LPS (18). However, macrophage activation and the severity of sepsis induced by i.p. injected LPS were not changed in Stab2 KO mice or in mice treated with the anti-Stab2 mAb (Figs. S2*E* and S4*C*). Furthermore, levels of inflammatory cytokines in serum and populations of various immune cells were not affected (Fig. S4 *A* and *B*). Therefore, inhibition of Stab2 function does not appear to directly affect the immune system. It is known that HA's functions depend on its molecular size, which varies from a few kDa to a few MDa (16). In the present study, HA molecules in Stab2 KO serum were ~40 kDa in size (Fig. S1*J*). possibly explaining some of the discrepancy between our results and those of previous studies.

Tumor cells circulate through the bloodstream and penetrate preferable tissues. Given that the s.c. proliferation of melanoma cells in Stab2 KO mice was not altered (Fig. 2*C*), we examined the initial step of attachment to the lungs. Melanoma cells expressing luciferase were injected via the tail vein, and cells trapped in the lungs were detected based on luciferase activity after perfusion with PBS to remove nonadherent cells. At 6 h after the i.v. injection, the number of melanoma cells trapped in the lungs was decreased in both the Stab2 KO mice and the mice given anti-Stab2, indicating that tumor metastasis is prevented at the initial stage of tissue penetration in the absence of Stab2 function (Fig. 5 *A* and *B*). Because those mice had extremely high plasma HA levels, we considered that the attachment of melanoma cells to the lungs is enhanced by HA displayed on the surface of blood vessels in normal lungs, and that a high level of HA in plasma blocks this interaction. In fact, melanoma cells adhered to HA-coated plates and pulmonary ECs, and HA at high concentrations, similar to those in serum of Stab2 KO mice, inhibited the attachment (Fig. 5, Fig. S3*F*, and Movies S1 and S2). Although i.v. injected HA is rapidly removed from the circulation, we found that the i.v. injection of a very high dose of HA was able to maintain the plasma HA concentration at a high level for at least 10 h (Fig. 5*C*). After the circulating HA level increased, B16F10 cells were injected to evaluate their attachment to the lungs. Metastasis of B16F10 cells to the lungs was markedly suppressed under these conditions (Fig. 3*D*). These results strongly suggest that inhibition of Stab2 function prevents tumor metastasis by elevating the plasma HA level.

Previous studies found that forced expression of HAS increased tumor cell proliferation and metastasis, whereas inhibition of HAS prevented proliferation and metastasis (23, 24, 30). These experiments suggested that HA promotes tumor proliferation and metastasis, whereas our results indicate that HA prevents metastasis. The critical difference between the previous studies and the present study is that we focused on the circulating HA, whereas most of the previous studies investigated extracellular matrix and pericellular HA. Therefore, it seems that the function of HA can differ depending on location.

In conclusion, our Stab2 KO mice were viable and exhibited no overt defects, but had dramatically increased plasma HA levels. This indicates that Stab2 is dispensable for normal development and homeostasis, and that an extremely high level of plasma HA has no deleterious effect. The increase in circulating HA levels was inversely correlated with metastasis and inhibited the attachment of melanoma cells to the lungs. Moreover, the administration of an anti-Stab2 mAb also increased the plasma HA level and blocked the metastasis of not only mouse melanoma cells, but also human breast tumor cells with no side effects. Thus, functional inhibition of Stab2 may be a potential strategy to suppress tumor metastasis.

Materials and Methods

A Stab2 KO mouse line was generated by conventional methods, as described in *SI Materials and Methods*, and backcrossed with C57BL/6 for at least six generations. Anti-mouse Stab2 mAb (#34-2) was generated in our laboratory (10). Serum HA levels were measured with an HA assay kit (Seikagaku Biobusiness) in accordance with the manufacturer's instructions. The cell internalization of FITC-HA into HSECs was performed as described previously (10). For FACS analysis, HSECs were incubated with indicated antibodies and FITC-HA, and labeled cells were analyzed with a FACSCalibur flow cytometer (BD Biosciences). B16F10 cells [5×10^5 (Fig. 2) or 5×10^4 (Fig. 3)] were injected into the tail vein. At 14 d after injection, the lung surface nodules were counted. For imaging in vivo, 5×10^5 B16F10-luc-G5 cells were injected i.v. At 7 d after the injection, metastasis was analyzed with luciferase luminescence as described previously (31). MDA-MB-231-luc-D3H2LN cells (4×10^6) were injected into the mammary gland of SCID mice, and metastasis was analyzed using the IVIS imaging system (31, 32). 4T1-LucNeo-1H cells (5×10^4) were injected into a mammary fad pad of SCID mice. Rolling and/or tethering of B16 melanoma cells onto cultured pulmonary ECs was analyzed under flow conditions at 0.7 dynes/cm^2 with the VenaEC System (Cellix) using confocal microscopy (Nikon A1R). Before the experiments, B16 melanoma cells were stained by CellTracker Red CMTPX (Molecular Probes) and Hoechst 33342 (Molecular Probes). Pulmonary ECs were also stained with CellTracker Green CMFDA (Molecular Probes) and Hoechst 33342. More detailed information is provided in *SI Materials and Methods*.

ACKNOWLEDGMENTS. We thank Dr. T. Akiyama for providing the B16F10 cells and Drs. H. Saya, T. Itoh, and M. Tanaka for valuable discussions and a critical reading of the manuscript. We also thank M. Tajima, C. Yoshinaga, and X. Yingda for their excellent technical help. This work was supported in part by research grants from the Ministry of Education, Culture, Sports, Science and Technology (MEXT) of Japan and the Ministry of Health, Labor and Welfare (MHLW) of Japan (to A.M.); the Centers of Research Excellence in Science and Technology program (A.M); the A-STEP program of the Japan Science and Technology Agency (Y.H.) and Takeda Science Foundation (to A.M.); the Funding Program for Next Generation World-Leading Researchers (to S.N.); the Japan Society for the Promotion of Science through its Funding Program for World-Leading Innovative Research and Development on Science and Technology (FIRST Program) (R.N.); Research Fellowships from a Grant-in-Aid 22113008 for Scientific Research on Innovative Areas of Fluorescence Live Imaging from The Ministry of Education, Culture, Sports, Science, and Technology of Japan (to S.N.); Grants-in-Aid for Scientific Research (to R.N.), grants for Translational Systems Biology and Medicine Initiative (to S.N. and R.N.), and the global Centers of Excellence program from the MEXT of Japan (R.N.); Banyu Life Science Foundation International (S.N.); and a research grant from the National Institute of Biomedical Innovation (to R.N.).

1. Fraser JR, Alcorn D, Laurent TC, Robinson AD, Ryan GB (1985) Uptake of circulating hyaluronic acid by the rat liver: Cellular localization in situ. *Cell Tissue Res* 242: 505–510.
2. Schledzewski K, et al. (2011) Deficiency of liver sinusoidal scavenger receptors stabilin-1 and -2 in mice causes glomerulofibrotic nephropathy via impaired hepatic clearance of noxious blood factors. *J Clin Invest* 121:703–714.
3. Politz O, et al. (2002) Stabilin-1 and -2 constitute a novel family of fasciclin-like hyaluronan receptor homologues. *Biochem J* 362:155–164.
4. Adachi H, Tsujimoto M (2002) FEEL-1, a novel scavenger receptor with in vitro bacteria-binding and angiogenesis-modulating activities. *J Biol Chem* 277:34264–34270.
5. Hansen B, et al. (2005) Stabilin-1 and stabilin-2 are both directed into the early endocytic pathway in hepatic sinusoidal endothelium via interactions with clathrin/AP-2, independent of ligand binding. *Exp Cell Res* 303:160–173.
6. Kzhyshkowska J, et al. (2005) Phosphatidylinositide 3-kinase activity is required for stabilin-1–mediated endosomal transport of acLDL. *Immunobiology* 210:161–173.
7. Kzhyshkowska J, et al. (2008) Alternatively activated macrophages regulate extracellular levels of the hormone placental lactogen via receptor-mediated uptake and transcytosis. *J Immunol* 180:3028–3037.
8. Kzhyshkowska J, et al. (2006) Novel function of alternatively activated macrophages: Stabilin-1-mediated clearance of SPARC. *J Immunol* 176:5825–5832.
9. Salmi M, Koskinen K, Henttinen T, Elima K, Jalkanen S (2004) CLEVER-1 mediates lymphocyte transmigration through vascular and lymphatic endothelium. *Blood* 104: 3849–3857.
10. Nonaka H, Tanaka M, Suzuki K, Miyajima A (2007) Development of murine hepatic sinusoidal endothelial cells characterized by the expression of hyaluronan receptors. *Dev Dyn* 236:2258–2267.
11. Park SY, et al. (2008) Rapid cell corpse clearance by stabilin-2, a membrane phosphatidylserine receptor. *Cell Death Differ* 15:192–201.
12. Gustafson S, Björkman T (1997) Circulating hyaluronan, chondroitin sulphate and dextran sulphate bind to a liver receptor that does not recognize heparin. *Glycoconj J* 14:561–568.
13. Harris EN, Weigel PH (2008) The ligand-binding profile of HARE: Hyaluronan and chondroitin sulfates A, C, and D bind to overlapping sites distinct from the sites for heparin, acetylated low-density lipoprotein, dermatan sulfate and CS-E. *Glycobiology* 18:638–648.
14. Kogan G, Soltés L, Stern R, Gemeiner P (2007) Hyaluronic acid: A natural biopolymer with a broad range of biomedical and industrial applications. *Biotechnol Lett* 29: 17–25.
15. Fraser JR, Laurent TC, Laurent UB (1997) Hyaluronan: Its nature, distribution, functions and turnover. *J Intern Med* 242:27–33.
16. Stern R, Asari AA, Sugahara KN (2006) Hyaluronan fragments: An information-rich system. *Eur J Cell Biol* 85:699–715.
17. Almond A (2007) Hyaluronan. *Cell Mol Life Sci* 64:1591–1596.
18. Jiang D, et al. (2005) Regulation of lung injury and repair by Toll-like receptors and hyaluronan. *Nat Med* 11:1173–1179.
19. DeGrendele HC, Estess P, Siegelman MH (1997) Requirement for CD44 in activated T cell extravasation into an inflammatory site. *Science* 278:672–675.
20. Zöller M (2011) CD44: Can a cancer-initiating cell profit from an abundantly expressed molecule? *Nat Rev Cancer* 11:254–267.
21. Banerji S, et al. (1999) LYVE-1, a new homologue of the CD44 glycoprotein, is a lymph-specific receptor for hyaluronan. *J Cell Biol* 144:789–801.
22. Kim S, et al. (2009) Carcinoma-produced factors activate myeloid cells through TLR2 to stimulate metastasis. *Nature* 457:102–106.
23. Sironen RK, et al. (2011) Hyaluronan in human malignancies. *Exp Cell Res* 317: 383–391.
24. Toole BP (2004) Hyaluronan: From extracellular glue to pericellular cue. *Nat Rev Cancer* 4:528–539.
25. Twarock S, et al. (2011) Inhibition of oesophageal squamous cell carcinoma progression by in vivo targeting of hyaluronan synthesis. *Mol Cancer* 10:30.
26. Kudo D, et al. (2004) Effect of a hyaluronan synthase suppressor, 4-methylumbelliferone, on B16F-10 melanoma cell adhesion and locomotion. *Biochem Biophys Res Commun* 321:783–787.
27. Zhou B, Weigel JA, Fauss L, Weigel PH (2000) Identification of the hyaluronan receptor for endocytosis (HARE). *J Biol Chem* 275:37733–37741.
28. Harris EN, Weigel JA, Weigel PH (2008) The human hyaluronan receptor for endocytosis (HARE/Stab2) is a systemic clearance receptor for heparin. *J Biol Chem* 283: 21453–21461.
29. Gale NW, et al. (2007) Normal lymphatic development and function in mice deficient for the lymphatic hyaluronan receptor LYVE-1. *Mol Cell Biol* 27:595–604.
30. Yoshihara S, et al. (2005) A hyaluronan synthase suppressor, 4-methylumbelliferone, inhibits liver metastasis of melanoma cells. *FEBS Lett* 579:2722–2726.
31. Takeshita F, et al. (2005) Efficient delivery of small interfering RNA to bone-metastatic tumors by using atelocollagen in vivo. *Proc Natl Acad Sci USA* 102:12177–12182.
32. Jenkins DE, Hornig YS, Oei Y, Dusich J, Purchio T (2005) Bioluminescent human breast cancer cell lines that permit rapid and sensitive in vivo detection of mammary tumors and multiple metastases in immune deficient mice. *Breast Cancer Res* 7:R444–R454.

SCIENTIFIC REPORTS

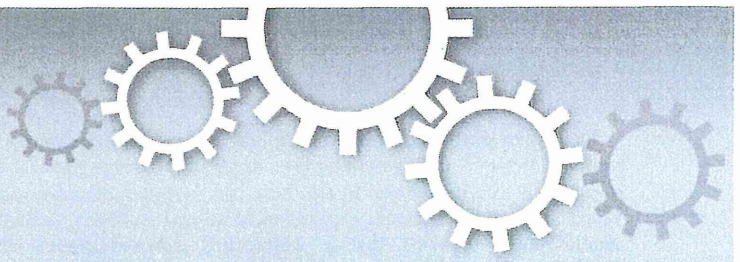

OPEN

SUBJECT AREAS:
NON-CONDING RNA'S
RNAI
SMALL RNA'S
TUMOUR SUPPRESSORS

Received
1 December 2011

Accepted
24 February 2012

Published
15 March 2012

Correspondence and requests for materials should be addressed to T.O. (tochiya@ncc.go.jp)

Stilbene derivatives promote Ago2-dependent tumour-suppressive microRNA activity

Keitaro Hagiwara[1,2], Nobuyoshi Kosaka[1], Yusuke Yoshioka[1], Ryou-u Takahashi[1], Fumitaka Takeshita[1] & Takahiro Ochiya[1,2]

[1]Division of Molecular and Cellular Medicine, National Cancer Center Research Institute, 5-1-1, Tsukiji, Chuo-ku, Tokyo 104-0045, Japan, [2]Department of Biological Sciences, Tokyo Institute of Technology, 4259 Nagatsuta-cho, Midori-ku, Yokohama 226-8501, Japan.

It is well known that natural products are a rich source of compounds for applications in medicine, pharmacy, and biology. However, the exact molecular mechanisms of natural agents in human health have not been clearly defined. Here, we demonstrate for the first time that the polyphenolic phytoalexin resveratrol promotes expression and activity of Argonaute2 (Ago2), a central RNA interference (RNAi) component, which thereby inhibits breast cancer stem-like cell characteristics by increasing the expression of a number of tumour-suppressive miRNAs, including miR-16, -141, -143, and -200c. Most importantly, resveratrol-induced Ago2 resulted in a long-term gene silencing response. We also found that pterostilbene, which is a natural dimethylated resveratrol analogue, is capable of mediating Ago2-dependent anti-cancer activity in a manner mechanistically similar to that of resveratrol. These findings suggest that the dietary intake of natural products contributes to the prevention and treatment of diseases by regulating the RNAi pathway.

Natural products are a rich source of valuable medicinal agents. More than half of the currently available drugs are natural or related compounds. In the case of cancer, the percentage of natural compounds exceeds 60%. Research on natural products as potential anti-cancer agents dates back to at least the Egyptian Ebers Papyrus of 1550 B.C. However, more recent scientific investigations began with the studies of Hartwell and co-workers on the application of podophyllotoxin and its derivatives as anti-cancer agents[1]. A large number of plant, marine, and microbial sources have been tested, and hundreds of active compounds have been isolated. Despite these advances, the underlying mechanisms of natural products in human health are not fully understood.

Resveratrol, which is a multi-functional polyphenolic compound, is a phytoalexin present in a wide variety of plant species, including grapes, mulberries, and peanuts[2]. Since its discovery, resveratrol has been shown to exhibit a plethora of physiological properties that may be useful in human medicine. More interest was focused on resveratrol at the beginning of the 1990s when it was first shown to be present in red wine[3]. Experimental studies have shown that resveratrol inhibits the growth of various cancer cells and induces apoptotic cell death[4,5]. Recently, a phase I/II clinical trial in patients with colon cancer was conducted to examine the effects of resveratrol treatment on colon cancer progression and colonic mucosa in patients with colon cancer and its effects in modulating the Wnt signalling pathway[2]. Although these data provide evidence of multiple anti-tumour effects induced by resveratrol, the exact mechanism is not clearly understood.

MicroRNAs (miRNAs) have emerged as key post-transcriptional regulators of gene expression that are involved in diverse physiological and pathological processes[6]. The inhibition of the miRNA biogenesis pathway results in severe developmental defects and lethality in many organisms[7]. It has been suggested that a considerable number of miRNAs have roles in cancer cells. Indeed, an increasing number of experimental studies have shown that the knock-down or the re-expression of specific miRNAs could induce drug sensitivity, inhibit the proliferation of cancer cells, and suppress cancer cell invasion and metastasis[8–10]. Recent studies have shown that natural products, including curcumin, isoflavone, I3C, DIM, and EGCG, could alter the expression of specific miRNAs, which may lead to the increased sensitivity of cancer cells to conventional anti-cancer agents and, therefore, tumour growth inhibition[11–14]. However, the exact molecular mechanism of miRNA induction and the biological significance of resveratrol-induced miRNAs have not been reported.

Diet is one of the most important modifiable cancer risk determinants[15]. Dietary components have been implicated in many pathways involved in carcinogenesis. In addition, carcinogenic processes are associated with the altered expression of several miRNAs. Recent studies have reported that a widespread down-regulation of miRNAs is commonly observed during human cancer-cell initiation and progression[16,17]. In this study, we hypothesised that the dietary intake of natural products maintains tumour-suppressive miRNA expression in cancer cells, leading to the prevention of carcinogenesis. We demonstrated that resveratrol suppresses cancer cell malignancy *in vitro* and *in vivo* through the transcriptional activation of tumour-suppressive miRNAs and Argonaute2 (Ago2). Furthermore, we provided evidence that Ago2 over-expression enhances the RNA interference (RNAi) activity. These findings suggest that the dietary intake of natural products safely reduces a wide range of negative consequences with an overall improvement in human health and survival by modulating miRNA biogenesis.

Results

Resveratrol reduces the cancer stem-like cells population by up-regulating miR-141 and miR-200c. To identify the potential anti-cancer activity of resveratrol, we investigated the effects of this compound on tumour formation *in vivo*. We orthotopically inoculated female SCID hairless outbred mice with MDA-MB-231-luc-D3H2LN cells (200 cells), which were then treated with resveratrol (25 mg/kg/day) or ethanol (control) via intraperitoneal injection every day for one week. Tumour growth was then monitored using an IVIS imaging system. The weight of the mice did not significantly change between the groups during the course of the experiment, suggesting that resveratrol did not have notable adverse effects on mice (Supplementary Fig. 1a). The results demonstrated that the resveratrol administration into the mice significantly suppressed tumour formation, while obvious tumours were observed in vehicle-treated mice, indicating that resveratrol is capable of inhibiting the survival and growth of cancer cells *in vivo* (Fig. 1a). A recent report has shown that solid tumours contain a distinct population of cells with the ability to form tumours in mice; these cells are known as tumour-initiating or cancer stem-like cells (CSCs) and display increased drug resistance and metastatic ability because they consistently form tumours, whereas other cancer cell populations were depleted of cells capable of tumour formation[18,19]. To identify the effects of resveratrol on the CSC phenotype, breast cancer cells were examined for changes in the CSC population, which is a highly tumourigenic $CD44^+/CD24^-$ subpopulation with stem cell-like self-renewal properties and the ability to produce differentiated progeny after resveratrol treatment[18]. Compared to vehicle-treated control cells, cells treated with 50 μM resveratrol demonstrated a significant 6-fold decrease in the $CD44^+/CD24^-$ population in MDA-MB-231-luc-D3H2LN cells (Fig. 1b). In addition, mammosphere formation, which has been widely used for breast CSC enrichment, of the $CD44^+/CD24^-$ fraction from MDA-MB-231-luc-D3H2LN cells was suppressed after resveratrol treatment (Supplementary Fig. 1b). We also assessed apoptosis using TUNEL staining and a caspase assay and found that resveratrol did not induce apoptosis (Supplementary Figs. 1c and 1d). Human breast cancers are driven by a CSC component that may contribute to tumour metastasis and therapeutic resistance[20]. Indeed, we found that the combination of resveratrol with low therapeutic doses of docetaxel elicits significantly greater cancer cell growth inhibition *in vitro* and *in vivo* (Supplementary Figs. 1e–g). These findings strongly suggest that resveratrol demonstrates multiple anti-cancer effects through the reduction of the CSC population.

To examine whether resveratrol could influence the breast cancer cell metastasis ability, the highly invasive breast cancer cell line MDA-MB-231-luc-D3H2LN was used in *in vitro* invasion assays. As shown in Fig. 1c, the invasion of MDA-MB-231-luc-D3H2LN cells was suppressed by resveratrol treatment. Previous studies have documented aberrant miRNA expression in cancer, and our observations prompted us to hypothesise that the anti-cancer resveratrol effects were mediated by miRNAs, particularly by a group of tumour-suppressive miRNAs[21]. A recent study has demonstrated that miR-141 and miR-200c strongly inhibit breast cancer invasion ability[22]. We found that resveratrol exposure increases miR-141 and miR-200c expression in MDA-MB-231-luc-D3H2LN cells (Fig. 1d). These findings suggest that resveratrol exhibits multiple anti-cancer effects through the inhibition of CSC phenotypes by activating miR-141 and miR-200c. In addition, to determine whether the up-regulation of miR-141 and miR-200c is mediated at the transcriptional level, we measured the expression levels of the primary miRNAs of miR-141 and miR-200c and found that these miRNAs are up-regulated at the primary transcript level (Supplementary Fig. 1h). Taken together, these results indicate that resveratrol increases the expression of tumour-suppressive miRNAs via the induction of miRNA transcription. Similar results were obtained in two other human breast cancer cell lines (MCF7 and MCF7-ADR) and MCF10A, an immortalised, non-transformed epithelial cell line (Supplementary Figs. 2–4).

Resveratrol up-regulates the expression of tumour-suppressive miRNAs. We demonstrated that resveratrol specifically reduced the CSC fraction (Fig. 1b). In addition, we also observed that miR-141 and miR-200c, which are known to suppress the CSC phenotype, are both induced by resveratrol treatment (Fig. 1d). These observations suggest that a part of the anti-cancer effects of resveratrol is mediated by miRNAs, particularly tumour-suppressive miRNAs. Indeed, a morphological change is observed after resveratrol treatment (Fig. 2a), suggesting that resveratrol induces a variety of miRNAs in cancer cells. To confirm whether miRNAs are globally up-regulated in the multiple anti-cancer effects induced by resveratrol in MDA-MB-231-luc-D3H2LN cells, we performed a comprehensive miRNA profiling of untreated MDA-MB-231-luc-D3H2LN cells and compared the results to those obtained in resveratrol-treated cells. As shown in Fig. 2b, we found that a subset of tumour-suppressive miRNAs is transcriptionally up-regulated by resveratrol (Table 1). To validate the microarray results, we performed qRT-PCR. A set of mature tumour-suppressive miRNAs, including miR-16 and miR-143, are significantly up-regulated in a variety of breast cancer cell lines, including MDA-MB-231-luc-D3H2LN, MCF7, MCF7-ADR, and MCF10A (Supplementary Figs. 2–5). These results indicated that resveratrol globally up-regulates tumour-suppressive miRNAs in human breast normal epithelial and cancer cells.

Resveratrol enhances the Ago2 RNAi potency. Although our data provide evidence that resveratrol globally up-regulates tumour-suppressive miRNAs and one of the mechanisms that is mediated by primary miRNA up-regulation, we also hypothesised that changes at other levels of the RNAi pathway may play a role in enhancing the resveratrol-mediated miRNA activity in cells in addition to transcriptional alterations. It is known that miRNA generation occurs in a multi-step process[23,24]. If one of the components associated with the miRNA pathway is under-expressed or qualitatively impaired, the pathway as a whole is destabilised. To examine the effect of resveratrol on the miRNA machinery, we measured the expression levels of a selected group of miRNA machinery-related genes, including Dicer1, Drosha, TARBP2, DGCR8, and Ago2, after the resveratrol treatment of MDA-MB-231-luc-D3H2LN cells. We found that resveratrol exposure significantly increased Ago2 expression in MDA-MB-231-luc-D3H2LN cells (Fig. 2c and Supplementary Fig. 6a). To elucidate the resveratrol-mediated Ago2 up-regulation mechanism, we assessed the Ago2 promoter activity and the Ago2 mRNA and protein half-lives after resveratrol treatment. As shown in supplementary Fig. 6b, the Ago2 protein half-lives were unchanged after resveratrol treatment. In contrast, the Ago2 mRNA was slightly